J|A|C|S ARTICLES

Published on Web 05/28/2010

Probing Electronic Superexchange Coupling at Isolated Poly-*p*-phenylene Molecules

Weihua Wang,[†] Shiyong Wang,[†] Xiuyuan Li,[†] Jean-Paul Collin,[‡] Jun Liu,[§] Pei Nian Liu,*[,§] and Nian Lin*[,†]

Department of Physics, The Hong Kong University of Science and Technology, Clear Water Bay, Hong Kong, China, Institut de Chimie, Université Louis Pasteur-CNRS/UMR 7177, 4, rue Blaise Pascal, 67070 Strasbourg, France, and Key Lab for Advanced Materials and Institute of Fine Chemicals, East China University of Science and Technology, Meilong Road 130, Shanghai, China

Received March 23, 2010; E-mail: phnlin@ust.hk; liupn@ecust.edu.cn

Abstract: Superexchange coupling in poly-*p*-phenylene molecular wires was probed using scanning tunneling microscopy/spectroscopy at cryogenic temperatures. The coupling strength was characterized by measuring the energy splitting between the molecular states constructed by symmetric and antisymmetric dimerization of molecular fragments' orbitals. The results confirm the theoretically predicted exponential decay behavior of the superexchange coupling on a single-molecule level. A decay constant of 0.10 ± 0.02 Å^{-1} was obtained. Owing to the high spatial resolution of scanning tunneling microscopy, the molecules' internal states (e.g., molecular conformation) as well as external states (e.g., interaction with foreign atoms or molecules) were elucidated with atomic precision at the mean time of characterizing the superexchange coupling. This method provides a new approach to quantify how intramolecular charge transfer is influenced by molecular conformation and interaction with the surroundings.

Introduction

Charge transfer (CT) in molecular wires is of fundamental importance in molecular electronics.[1,2] Theoretically CT is described by a superexchange mechanism for short molecules under "off-resonance" conditions.[3] Experimentally, two properties, the molecular conductance and the kinetic charge transfer rate, are measured to characterize intramolecular CT processes.[1−5] For a fair comparison between theory and experiment, not only measurements on individual molecules are required but also the molecular internal (e.g., molecular conformation) and external status (e.g., molecular interaction with contact electrodes or solvent molecules) should also be accurately determined in atomic-scale detail, because these parameters may affect the results decisively. These requirements pose daunting experimental challenges due to the minute size of single molecules. Recently, scanning tunneling microscopy has been used to measure single-molecule conductance owing to its ability to manipulate or contact single molecules.[6−8] However, in those experiments, neither the molecular conformation nor the contact structure was unambiguously determined. In this study, we demonstrated an approach to characterizing the charge transfer phenomena of isolated molecules, whose internal and external states are well-defined, by means of scanning tunneling microscopy/spectroscopy (STM/STS). Instead of directly addressing molecular conductance or kinetic rate constants, we measured the superexchange coupling of single molecules using STM techniques at cryogenic temperatures. At the same time, we precisely determined the molecules' conformation and the surrounding conditions in atomic-scale detail. Our results confirm, on a single-molecule level, the theoretically predicted

[†] The Hong Kong University of Science and Technology.
[‡] Université Louis Pasteur-CNRS/UMR 7177.
[§] East China University of Science and Technology.

(1) (a) Weiss, E. A.; Wasielewski, M. R.; Ratner, M. A. *Top. Curr. Chem.* **2005**, *257*, 103. (b) Aviram, A.; Ratner, M. A. *Chem. Phys. Lett.* **1974**, *29*, 277. (c) *Molecular Electronics: Science and Technology*; Aviram, A., Ratner, M., Eds.; New York Academy of Sciences: New York, 1998.
(2) (a) Nitzan, A.; Ratner, M. A. *Science* **2003**, *300*, 1384. (b) Xue, Y.; Datta, S.; Ratner, M. A. *J. Chem. Phys.* **2001**, *115*, 4292.
(3) Joachim, C.; Ratner, M. A. *Nanotechnology* **2004**, *15*, 1065, and the references therein.
(4) (a) Joachim, C.; Gimzewski, J. K.; Aviram, A. *Nature* **2000**, *408*, 541. (b) Tao, N. J. *Nat. Nanotechnol.* **2006**, *1*, 173. (c) Nitzan, A. *Annu. Rev. Phys. Chem.* **2001**, *52*, 681.
(5) For example, see: (a) Chen, J.; Wang, W.; Reed, M. A.; Rawlett, A. M.; Price, D. W.; Touret, J. M. *Appl. Phys. Lett.* **2000**, *77*, 1224. (b) Datta, S.; Tian, W.; Hong, S.; Reifenberger, R.; Henderson, J. J.; Kubiak, C. P. *Phys. Rev. Lett.* **1997**, *79*, 2530. (c) Joachim, C.; Gimzewski, J. M.; Schlittler, R. R.; Chavy, C. *Phys. Rev. Lett.* **1995**, *74*, 2102. (d) Reed, M. A.; Zhou, C.; Muller, C. J.; Burgin, T. P.; Tour, J. M. *Science* **1997**, *278*, 252. (e) Gonzalez, M. T.; Wu, S. M.; Huber, R.; van der Molen, S. J.; Schonenberger, C.; Calame, M. *Nano Lett.* **2006**, *6*, 2238. (f) Seferos, D. S.; Trammell, S. A.; Bazan, G. C.; Kushmerick, J. G. *Proc. Natl. Acad. Sci. U.S.A.* **2005**, *102*, 8821. (g) Yazdani, A.; Eigler, D. M.; Lang, N. D. *Science* **1996**, *272*, 1921. (h) Temirov, R.; Lassise, A.; Anders, F. B.; Tautz, F. S. *Nanotechnology* **2008**, *19*, 6065401. (i) Cui, X. D.; Primak, A.; Zarate, X.; Tomfohr, J.; Sankey, O. F.; Moore, A. L.; Moore, T. A.; Gust, D.; Harris, G.; Lindsay, S. M. *Science* **2001**, *294*, 571.
(6) Lafferentz, L.; Ample, F.; Yu, H.; Hecht, S.; Joachim, C.; Grill, L. *Science* **2009**, *323*, 1193.
(7) Kockmann, D.; Poelsema, B.; Zandvliet, H. J. W. *Nano Lett* **2009**, *9*, 1147.
(8) Haiss, W.; Wang, C. S.; Grace, I.; Batsanov, A. S.; Schiffrin, D. J.; Higgins, S. J.; Bryce, M. R.; Lambert, C. J.; Nichols, R. J. *Nat. Mater.* **2006**, *5*, 995.

 10.1021/ja102415f

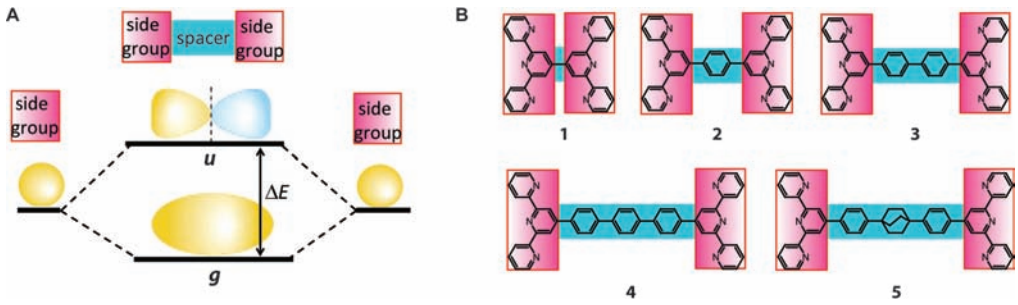

Figure 1. (a) Schematic illustration of the orbital diagram of a molecule of topology $\sigma-\phi-\sigma$. The orbitals of two identical side groups construct an *s*-like symmetric orbital (*g*) at a low energy and a *p*-like antisymmetric orbital (*u*) at a high energy as the two groups are linked by a spacer. (b) Bis-terpyridine poly-*p*-phenylene compounds (**1**−**4**) and bis-terpyridine bicyclo[2.2.2]octane (**5**) used in this study.

exponential decay of superexchange coupling and we were able to derive a decay constant of 0.10 ± 0.02 Å^{-1} for poly-*p*-phenylene systems.

At the extended Hückel level, the electronic superexchange coupling V_{ab} of two symmetric (degenerate) systems can simply be taken as half of the energy splitting between two dimerized orbitals having antisymmetric and symmetric symmetry under off-resonance conditions.[9−11] As illustrated in Figure 1a, in a molecule of a $\sigma-\phi-\sigma$ topology (σ stands for a side group and ϕ stands for a spacer), an *s*-like orbital (denoted as *g*) is constructed by a symmetric combination of the orbitals of the two side groups and a *p*-like orbital (denoted as *u*) is constructed by an antisymmetric combination of the same orbitals. The *s*-like orbital is at a low energy while the *p*-like orbital is at a high energy. In particular, under the conditions that the molecular states of σ and ϕ are off in energy and the molecular states of σ are localized, the energy splitting ($\Delta E = E_u - E_g$) represents the strength of the superexchange coupling, $\Delta E \propto V_{ab}$. In this study, we have chosen bis-terpyridine poly-*p*-phenylene molecules as the model system. As shown in Figure 1b, each compound consists of two terpyridine (*tpy*) units as the side groups and a poly-*p*-phenylene ($(ph)_n$, n = 0, 1, 2, 3) as the spacer group.

Methods

The experiments were carried out in an ultrahigh vacuum scanning tunneling microscope system (Omicron) operated at 4.9 K. A Cu(111) single crystal was cleaned by cycles of Ar ion sputtering and annealing. The molecules were thermally evaporated onto the Cu(111) substrate held at 180 K or room temperature. The evaporation temperatures for compounds **1** to **5** are approximately 520, 570, 590, 630, and 660 K, respectively. Samples were prepared with low molecule coverage, so that it was easy to find single molecules on Cu terraces. The STM topograph data were acquired in constant current mode. The d*I*/d*V* signals were measured using a lock-in amplifier with a sine modulation of 2 kHz at 18.3 mV. To improve the signal-to-noise ratio at low bias voltage and avoid molecular modification by the high current at high bias voltage, the spectra were acquired in a varied *Z* mode, in which the tip height *Z* changes as a function of *V* during the measurements. ($Z(V) = Z_0 + \Delta Z + \alpha|V|$, where Z_0 is the initial tip height given by the set point, ΔZ is the tip offset, and α is the change parameter.) The d*I*/d*V* − *V* spectra were measured at a set point of −0.2 V and 0.5 nA, with ΔZ = 0.06 nm and α = 0.02 nm/V. Some of the spectra were the average of the spectra measured along the dashed lines in Figure 3a.

Quantum chemistry calculations of free molecules were performed using Gaussian software (Gaussian 03) by Hartree-Fork (HF 6-31g) and density functional theory (DFT B3LYP/6-31 g) methods. In addition, molecules of coplanar molecular conformation (i.e., the dihedral angles of the free molecules were set to zero) were also calculated. The DFT calculated frontier molecular orbitals (MOs) of *tpy* as well as various poly-*p*-phenylene compounds (all in coplanar conformation) are shown in Supporting Information Figure S1. The surface was not included in the calculations. To estimate the influence of the surface, we have studied a terpyridine molecule adsorbed on the Cu(111) surface by density functional calculations (VASP).[12] The calculations verify that the terpyridine is physisorbed weakly on the surface with a molecule-to-surface separation of 3.5 Å. The calculations also confirm that the intrinsic molecular states are largely preserved with such a weak interaction, and no hybridization states are formed. We did not carry out similar calculations for the full molecules. However, we do not expect the nature of the molecule-to-surface interaction for the full molecules will be significantly different since the bridging poly-*p*-phenylene system is known to interact weakly, dominated by van der Waals forces, with noble metal (111) surfaces.[13]

Results and Discussion

First, as a reference, we have characterized a terpyridine-biphenylene (*tpy-bph*) compound (molecular structure shown in Figure 2a). Figure 2a shows an STM topograph of an isolated *tpy-bph* molecule adsorbed on a defect-free Cu(111) surface in a flat-lying configuration. Figure 2b shows the site-dependent d*I*/d*V*-*V* spectra, i.e., spectra acquired at the *tpy* site and the *bph* site. In the measurement range of −2.2 V to +2.2 V, one broad peak at 1.22 V was detected at the *tpy* site and one narrow peak at 2.03 V at the *bph* site. The broad peak can be fitted by two Gaussian peaks at 1.13 and 1.53 V, as shown by the dashed curves in Figure 2b. The site-dependence can be attributed to localized states. Figure 2c reproduces the STS maps (or d*I*/d*V* maps) at the energies of interest, which clearly show that the two low-energy states are localized at the *tpy* and the high-energy state is localized at the *bph*. Calculations suggest that the two components (1.13 and 1.53 V) of the low-energy peak can be ascribed as LUMO and LUMO+1 and the high-energy peak of 2.03 V as LUMO+2 (see Supporting Information Figure S2).

Since the 1.13-V and 1.53-V states are well separated from the 2.03-V state in energy and highly localized at *tpy*, the off-resonance conditions are fulfilled when two *tpy* groups are linked

(9) Joachim, C.; Launay, J. P.; Woitellier, S. *Chem. Phys.* **1990**, *147*, 131.
(10) Calzado, C. J.; Malrieu, J. P.; Sanz, J. F. *J. Phys. Chem. A* **1998**, *102*, 3659.
(11) Patoux, C.; Launay, J. P.; Beley, M.; Chodorowski-Kimmes, S.; Collin, J. P.; James, S.; Sauvage, J. P. *J. Am. Chem. Soc.* **1998**, *120*, 3717.
(12) Shi, X.; Zhang, R. Q.: Minot, C.;. Hermann, K.; Van Hove M.; Wang, W.; Lin, N. In preparation.
(13) (a) Witte, G.; Lukas, S.; Bagus, P. S.; Woll, C. *Appl. Phys. Lett.* **2005**, *87*, 263502. (b) Bagus, P. S.; Hermann, K.; Woll, C. *J. Chem. Phys.* **2005**, *123*, 184109. (c) Nguyen, M.-T.; Pignedoli, C. A.; Treier, M.; Fasel, R.; Passerone, M. *Phys. Chem. Chem. Phys.* **2010**, *12*, 992.

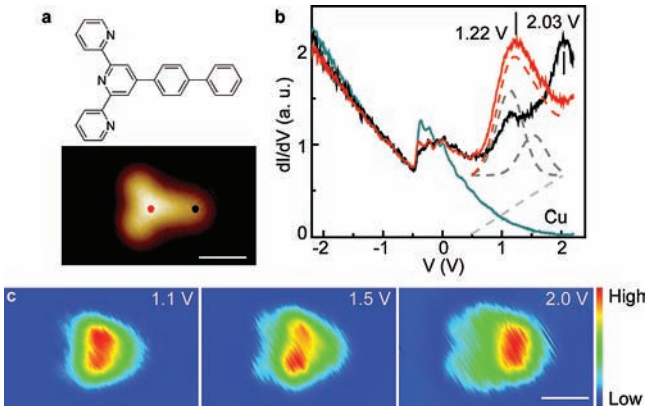

Figure 2. (a) Molecular structure and STM topograph of *tpy-bph* molecule (not to scale). (b) Site-dependent dI/dV−V spectra acquired at the *tpy* site (red dot) and the *bph* site (black dot), respectively. The fitting of the 1.22-V peak is illustrated by the dashed curves showing a 1.13-V peak, a 1.53-V peak and a linear background (the red dashed curve is the superposition of the three components). (c) STS maps at the indicated energies showing the two low-energy states are concentrated at *tpy* and the high-energy state at *bph* (scale bars in (a) and (c): 1 nm; imaging conditions: −0.2 V and 0.5 nA).

by a poly-*p*-phenylene spacer to comprise a *tpy*-(*ph*)$_n$-*tpy* molecule. Hence, for molecules of such topology, the energy splitting between the symmetric and antisymmetric dimerized states can be used to measure the superexchange coupling through the bridging (*ph*)$_n$ spacer. Figure 3a shows STM topographs of *tpy*-(*ph*)$_n$-*tpy* molecules with n = 0, 1, 2, and 3 (compounds **1**, **2**, **3**, and **4**). The apparent dimension in the molecules' axial direction (along the poly-*p*-phenylene spacer) ranges from 1.5 to 3.0 nm, reflecting different spacer lengths. We selected the molecules that were adsorbed in isolation as the target molecules in our measurements; i.e., they did not contact other molecules or surface defects (for instance, atomic steps).

The tunneling spectra acquired at single molecules of compounds **1** to **4** also exhibit site-dependence. Figure 3b shows the site-dependent dI/dV − V spectra, and Figure 3c shows representative STS maps at the indicated energies for each compound. For compound **1**, a narrow peak appeared at 0.55 V showing a symmetric spatial distribution maximized at the molecular center. The blue/red spectrum exhibits a narrow peak at 0.55 V and a broad peak at 1.55 V. It is known that measured molecular electronic states are broadened by temperature and measurement parameters (modulation voltage used in lock-in amplifier). Under the same experimental conditions, this broadening is identical for different states; i.e., the peaks in the same spectrum should possess a very similar width which can be quantified by full width at half maximum (fwhm). The narrow peak at 0.55 V can be fitted by a single Gaussian peak with fwhm = 0.48 V. Using a similar value of fwhm, the broader peak at 1.55 V can be fitted by two Gaussian peaks at 1.30 and 1.72 V. The overall fitted curve is shown by the dashed blue curve, which nicely reproduces the experimental spectra. STS mapping reveals that the 1.7-V component has a saddle-like shape showing double maxima at the two flanks of the molecule. Like compound **1**, compound **2** has a narrow low-energy (1.15 V) peak and a broad high-energy peak consisting of a shoulder at 1.35 V and a peak at 1.64 V. In the STS maps, the low-energy state of compound **2** shows a symmetric spatial distribution maximized at the molecular center, similar to the low-energy state of compound **1**, while the high-energy state shows

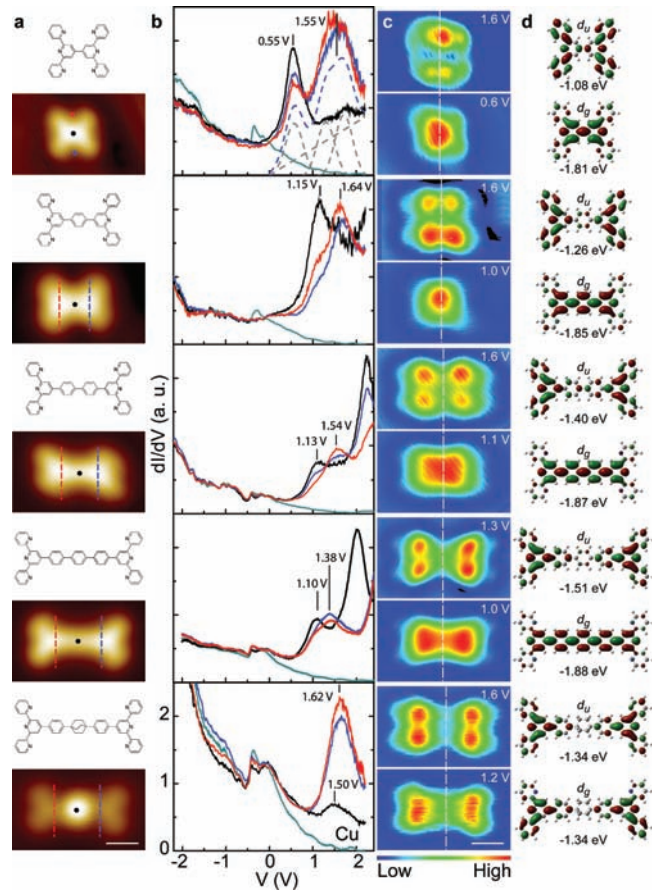

Figure 3. (a) Molecular structure and single-molecule STM topograph (not to scale with the molecular structure) of compound **1**, **2**, **3**, **4**, and **5** from top to bottom. (b) Site-dependent tunneling spectra (dI/dV − V) acquired at the indicated sites in (a) (following color code) for each molecule. For compound **1**, as an example, the blue spectrum is fitted by three peaks at 0.57, 1.30, and 1.72 V with the same fwhm (0.48 V) (the blue dashed curve is the superposition of the three components and a linear background). (c) STS maps at the indicated energies for each compound, showing the *s*-like states at low energy and *p*-like states at high energy for compounds **1** to **4**. The dashed lines indicate the molecular reflection plane (scale bars in (a) and (c): 1 nm; imaging conditions: −0.2 V and 0.5 nA for compounds **1**, **3**, **4**, and **5**, 0.8 V and 0.5 nA for compounds **2**). (d) Calculated wave function and energy of d_g and d_u orbitals for each compound.

a pair of double maxima that are distributed symmetrically with respect to the reflection plane which bisects the molecule (indicated by the dashed line in Figure 3c). We have observed very similar characteristics for compounds **3** and **4** (cf. Figure 3). In addition, at the central position, compound **3** or **4** shows a peak of ∼2.0 V which, according to its energy and shape, can be ascribed to the state of the central poly-*p*-phenylene group. Overall, the common feature of the four compounds is that each possesses a low-energy state of appreciable intensity in the middle and a high-energy state of deficient intensity in the middle. (Note, though, that for compound **1** only the lower side shows this feature clearly, presumably due to its small size.) Since, at positive bias voltages, electrons flows from the STM tip into the molecules, these states represent empty molecular orbitals. The contribution of vibronic states is excluded because according to literature molecular vibronic states were not detectable when molecules were adsorbed on metallic surface.[14]

The origin of these observed states can be elucidated by calculations. As seen in Supporting Information Figures S3−S6, as the two *tpy* groups are linked by a poly-*p*-phenylene spacer, their LUMO+1 orbitals can effectively form dimerized

orbitals at well-separated energies (let d_g and d_u denote the symmetric and antisymmetric orbitals, respectively, following the orbitals' D_{2h} symmetry). Figure 3d shows the wave functions and energies of the d_g and d_u orbitals for each compound obtained by DFT calculations (in coplanar conformation). The low-energy d_g orbitals are mostly distributed at the poly-*p*-phenylene group with a symmetric (*s*-like) shape. (The calculations excluded the contribution from the poly-*p*-phenylene states to the d_g orbitals. See Supporting Information Figure S7.) The high-energy d_u orbitals are mostly distributed at the two side *tpy* groups with a nodal plane (perpendicular to the molecular axis) in the wave functions, giving them a *p*-like shape. Since the STS maps reflect the distribution of local density of the states, which is proportional to the squares of their wave functions, the experimentally observed intensity deficit at the molecule's middle plane (cf. Figure 3c) can be attributed to the wave functions of these states having a planar node in the middle. In other words, they are *p*-like states. Based on the orbital shape and energy, the experimentally observed high-energy (low-energy) states can be assigned to the *p*-like (*s*-like) antisymmetric (symmetric) d_u (d_g) orbitals. (Note that, for compound **1**, the higher-energy component at 1.72 V of the broader peak is assigned as the *p*-like state based on the fact that its spatial distribution and its energy level resemble the features of the d_u state). According to the extended Hückel model, the energy splitting between these two states can be used to quantify the superexchange coupling strength of the poly-*p*-phenylene bridges.[15] Hence, these results allow us to understand how the superexchange coupling varies with the different spacers. It is worthwhile to note the dimerized states constructed by the *tpy*'s LUMO orbitals shown in Supporting Information Figure S3−S6 may be attributed to the lower-energy components of the broader peaks (cf. Figure 3b).

In a control experiment, we have studied a molecule (compound **5**) in which two *tpy* groups are linked by a nonconjugated (bicyclo[2.2.2]octane) spacer, as shown in the bottom panel of Figure 3a. In the STS spectra, the side sites show a peak at 1.62 V and the central site shows a peak at 1.50 V but with a much lower intensity (Figure 3b, bottom). The STS maps at 1.6 and 1.2 V are shown in Figure 3c (bottom). Obviously, unlike the previous molecules, compound **5** does not have a low-energy *s*-like state. Therefore the two *tpy* groups of compound **5** can be viewed as two units that are chemically linked but electronically decoupled. Calculations support this view. Figure 3d (bottom) shows that both the antisymmetric and symmetric dimerized orbitals of compound **5** are localized at the two *tpy* groups. These two states are degenerate (i.e., there is no energy splitting between the d_g and d_u orbitals), which indicates an absence of superexchange coupling. Since the spacer of **5** is of a similar length as that of **4**, the sharp contrast between **4** and **5** implies that the nonconjugated spacer effectively suppresses superexchange coupling. Furthermore, the absence of the antisymmetric and symmetric states implies that coupling through Cu surface electrons can be neglected.

The energy splitting ΔE between the *s*-like state and the *p*-like state of compounds **1** to **4** is plotted as a function of n in Figure 4 in a semilog scale. For each compound, several molecules were examined in multiple measurements (8−23 examples for various compounds) and ΔE varies in a range, as indicated by the error bar in Figure 4. This variation of ΔE may be caused by subtle molecular conformation differences of individual molecules, for example, different dihedral angles, because the energy splitting is very sensitive to molecular conformation. Considering the effective length of 4.3 Å per phenylene unit, the experimental data can be well fitted by an exponential decay $\Delta E \propto \exp(-kd)$ with a decay constant of 0.10 ± 0.02 Å^{-1}. As discussed before, the energy splitting is proportional to superexchange coupling V_{ab} ($\Delta E \propto V_{ab}$); we conclude that in the poly-*p*-phenylene systems, superexchange coupling decays with a rate of 0.10 ± 0.02 Å^{-1}. The DFT calculations support this trend as the calculated energy splitting exhibiting exponential decay behavior too, at a rate of 0.08 Å^{-1} (0.05 Å^{-1}) for the twisted (coplanar) molecules.

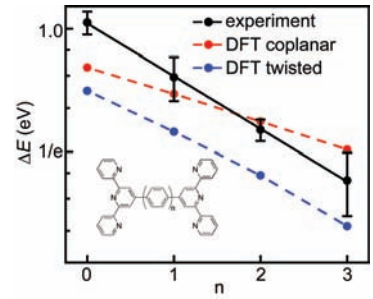

Figure 4. The measured and the calculated energy splitting ΔE between the symmetric *s* state and antisymmetric *p* state for compounds **1**, **2**, **3**, and **4** as a function of number of phenylene unit (*n*). The exponential fitting of the measured values (solid line) obtains a decay constant of 0.10 ± 0.02 Å^{-1}. The exponential fitting of the calculated values obtains a decay constant of 0.08 Å^{-1} (0.05 Å^{-1}) for the twisted (coplanar) molecules.

Exponential decay is generally found in measurements of ensembles of molecules for superexchange coupling, as well as in intramolecular CT rate constants or molecular conductance in the superexchange regime. The rate constant k_{DA} of the nonadiabatic CT from a donor to an acceptor is $k_{DA} = 2\pi/\hbar |V_{DA}|^2$ FCWD, where V_{DA} is the donor−acceptor coupling matrix element and FCWD is the Franck−Condon weighted density of states.[1,16] Recent work has established a relation between the CT rate constant and direct conductance *g* across a molecule as $g \approx (e^2/FCWD)k_{DA}$.[17,18] So, both k_{DA} and *g* are expected to decay with a decay constant of twice that of V_{DA}. To the first approximation, superexchange coupling V_{ab} decays at the same rate as the donor−acceptor coupling V_{DA}.[1,5,15] Thus we can compare our result with intramolecular CT as well as direct conductance. Table 1 summarizes the decay constants of the poly-*p*-phenylene systems obtained in this study along with those obtained using other methods. The superexchange coupling decays at a rate of 0.118 Å^{-1} or 0.19 Å^{-1},[15,19] which is in fair agreement with our result. For the rate constants or molecular conductance, taking into account the factor of 2, the experimentally obtained decay constants are larger than our value. A likely reason for this discrepancy is that the poly-*p*-phenylene spacers in those studies were in a free molecular conformation with a twisted dihedral angle, while in our experiment the molecules were in a conformation in which the dihedral angle was reduced.[20,21] Although the actual dihedral angle is unknown

(14) (a) Pradhan, N. A.; Liu, N.; Ho, W. *J. Phys. Chem. B* **2005**, *109*, 8513. (b) Qiu, X. H.; Nazin, G. V.; Ho, W. *Phys. Rev. Lett.* **2004**, *92*, 206102.
(15) Launay, J. P. *Chem. Soc. Rev.* **2001**, *30*, 386.
(16) Ratner, M. A. *J. Phys. Chem.* **1990**, *94*, 4877.
(17) Nitzan, A. *J. Phys. Chem. A* **2001**, *105*, 2677.
(18) Berlin, Y. A.; Ratner, M. A. *Radiat. Phys. Chem.* **2005**, *74*, 124.
(19) Weiss, E. A.; Ahrens, M. J.; Sinks, L. E.; Gusev, A. V.; Ratner, M. A.; Wasielewski, M. R. *J. Am. Chem. Soc.* **2004**, *126*, 5577.
(20) Venkataraman, L.; Klare, J. E.; Nuckolls, C.; Hybertsen, M. S.; Steigerwald, M. L. *Nature* **2006**, *442*, 904.

Table 1. Decay Constant of Poly-*p*-phenylene Systems Obtained in This Work and Literature

Property	Decay Constant, $Å^{-1}$	Method Reference
V_{ab} (Superexchange coupling)	0.10 ± 0.02	Energy splitting of dimerized states this work
	0.118	Intervalence transitions[15]
	0.19	Magnetic exchange[19]
$k_{DA}/2$ (CT kinetic rate constant)	0.16	Luminescence1[22]
	0.23	Transient absorption[19]
	0.33	Transient absorption[19]
$g/2$ (Molecular conductance)	0.18	AC voltammetry[23]
	0.30	Ag-SAM/STM-Hg[24]
	0.18−0.25	C-AFM[25]
	0.21	C-AFM[26]
	0.17	STM break junction[20]
	0.13 (twisted) 0.08 (planar)	DFT-Green function[27]
	0.16 (twisted) 0.12 (planar)	NEGF-DFT[28]
	0.26 (twisted) 0.20 (planar)	NEGF-DFT[29]
	0.14 (planar)	ESQC[30]
	0.17 (twisted)	DFT+Σ[31]
	0.18 (twisted)	NEGF-DFT[32]

based on STM topographs, it is a general view that the dihedral angle is reduced by molecule-to-surface interaction when molecules are adsorbed on a metal surface. For example, a recent report concluded that the dihedral angle of a poly-*p*-phenylene molecule is reduced from 30° in the gas phase to 16° upon its adsorption on a Au(111) surface.[13c] It was predicted that the conjugation of poly-*p*-phenylene molecular wires is effectively enhanced in a coplanar conformation resulting in smaller decay constants.[27−29] One can see our result of 0.10 ± 0.02 $Å^{-1}$ agrees well with the calculated values of coplanar wires reported in the literature.

Conclusions

We have presented an effective experimental approach to investigate the intramolecular CT phenomena of isolated molecules while at the same time imaging their conformation and precisely determining their surrounding conditions in atomic-scale detail. We have characterized superexchange coupling at individual molecules by measuring the energy splitting between the symmetric and antisymmetric states constructed by dimerization of the molecular fragments' orbitals. Because of its ability to determine the molecules' internal/external status precisely, this method opens the door to investigate how superexchange coupling, and in a broader sense intramolecular CT or molecular conductance, is influenced by molecular conformation or contacts with the surroundings, which is otherwise difficult to address directly. Finally, we discuss the applicability of our method. For a molecular wire of low conductance, the superexchange coupling is weak, so the energy splitting is small. If this value is below the experimental detection limit, our approach is not applicable. Therefore, in principle, our approach is more suitable to detect molecular wires of good conductivity, such as conjugated polymers of poly-*p*-phenylene, poly-phenyl-ethylene, or poly(*p*-phenylene vinylene).

Acknowledgment. This work was supported financially by Grant RPC07/08.SC11 from the Hong Kong University of Science and Technology, by the NSFC (Project No. 20902020), and by the Shanghai Pujiang Talent Program (Project No. 09PJ1403500).

Note Added after ASAP Publication. In the version published ASAP May 28, 2010, Figure 4 and the TOC graphic contained errors; the correct version reposted June 3, 2010.

Supporting Information Available: Synthesis. Supporting Figures. This material is available free of charge via the Internet at http://pubs.acs.org.

JA102415F

(21) Mishchenko, A.; Vonlanthen, D.; Meded, V.; Bürkle, M.; Li, C.; Pobelov, I. V.; Bagrets, A.; Viljas, J. K.; Pauly, F.; Evers, F.; Mayor, M.; Wandlowski, T. *Nano Lett* **2010**, *10*, 156.
(22) Schlicke, B.; Belser, P.; De Cola, L.; Sabbioni, E.; Balzani, V. *J. Am. Chem. Soc.* **1999**, *121*, 4207.
(23) Creager, S.; Yu, C. J.; Bamdad, C.; O'Connor, S.; MacLean, T.; Lam, E.; Chong, Y.; Olsen, G. T.; Luo, J. Y.; Gozin, M.; Kayyem, J. F. *J. Am. Chem. Soc.* **1999**, *121*, 1059.
(24) Holmlin, R. E.; Haag, R.; Chabinyc, M. L.; Ismagilov, R. F.; Cohen, A. E.; Terfort, A.; Rampi, M. A.; Whitesides, G. M. *J. Am. Chem. Soc.* **2001**, *123*, 5075.
(25) Ishida, T.; Mizutani, W.; Aya, Y.; Ogiso, H.; Sasaki, S.; Tokumoto, H. *J. Phys. Chem. B* **2002**, *106*, 5886.
(26) Wold, D. J.; Haag, R.; Rampi, M. A.; Frisbie, C. D. *J. Phys. Chem. B* **2002**, *106*, 2813.
(27) Kondo, M.; Tada, T.; Yoshizawa, K. *J. Phys. Chem. A* **2004**, *108*, 9143.
(28) Liu, H. M.; Wang, N.; Zhao, J. W.; Guo, Y.; Yin, X.; Boey, F. Y. C.; Zhang, H. *ChemPhysChem* **2008**, *9*, 1416.
(29) Kaun, C. C.; Larade, B.; Guo, H. *Phys. Rev. B* **2003**, *67*, 121411.
(30) Magoga, M.; Joachim, C. *Phys. Rev. B* **1997**, *56*, 4722.
(31) Quek, S. Y.; Choi, H. J.; Louie, S. G.; Neaton, J. B. *Nano Lett* **2009**, *9*, 3949.
(32) Cohen, R.; Stokbro, K.; Martin, J. M. L.; Ratner, M. A. *J. Phys. Chem. C* **2007**, *111*, 14893.